Neuroradiology (2012) 54:849–855
DOI 10.1007/s00234-011-0984-6

INTERVENTIONAL NEURORADIOLOGY

# Effects of metal coverage rate of flow diversion device on neointimal growth at side branch ostium and stented artery: an animal experiment in rabbit abdominal aorta

**Bo Hong · Kuizhong Wang · Qinghai Huang · Yi Xu · Xinggen Fang · Zhen Li · Jianmin Liu**

Received: 28 August 2011 / Accepted: 21 November 2011 / Published online: 15 December 2011


**Abstract**
*Introduction* To access the effect of actual metal coverage rate (MCR) on neointimal growth at covered side branch ostium and stented artery after implantation of a flow diversion device.
*Methods* Flow diverters (FDs) were implanted into abdominal aortas of 20 New Zealand rabbits. Four weeks and three months after FD implantation, the patency of side branches covered by the devices was assessed by angiography. The animals were sacrificed after angiography at 3 months post-surgery. The local actual MCR was measured under microscope and calculated. The extent of neointimal coverage at the ostia of branches and the neointima within the stent were examined by histology and scanning electron microscopy.
*Results* No side branch occlusion was noted, either immediately after implantation or at follow-ups. At 3 months after implantation, the intimal coverage of branch ostia caused by a 30–40% MCR was not significantly different from that caused by an MCR≤30% ($p$=0.792), but it was significantly lower than that caused by an MCR≥40% ($p$=0.021). Neointimal thickness in the stented abdominal aorta was positively correlated to MCR ($r$=0.523, $p$=0.001). The neointima was composed predominantly of smooth muscle cells and collagen fibers.
*Conclusion* The actual MCR exhibited remarkable differences once FD was implanted in vivo. Significantly more intimal coverage at the side branch ostia could be induced when MCR was ≥40%. The neointimal thickness within the stent was positively correlated to device MCR.

**Keywords** Flow diverter · Metal coverage rate · Abdominal aorta · Side branch · Neointima

## Introduction

Flow diversion devices are designed to alter flow dynamics and, even without coils, induce cerebral aneurysm occlusion. Recently, several investigators have reported successful treatment results using flow diverters (FDs), either in experiments or in clinical application [1–28]. One concern of using this device to treat intracranial aneurysms is whether it may lead to stenosis or occlusion of side branches or perforators once covered with dense metal mesh. Infarction caused by side branch or perforator occlusion has been reported [13, 20, 26, 28]; however, only few studies have paid due attention to this issue [10, 11, 22], and no calculations were made with regard to the actual metal coverage rate (MCR). During implantation procedure, FD can be either compressed or stretched, affecting its MCR significantly. In this study, we implanted FDs into rabbit abdominal aortas, covering side branches. The patency of side branch covered by FD was evaluated by angiography at 4 weeks and 3 months after implantation. Actual MCR, extent of neointimal formation covering the ostia of side branches were examined by histology and scanning electron microscopy (SEM). Their correlations as well as the neointimal thickness within the stented parent artery were also assessed.

Dr. Kuizhong Wang and Bo Hong are co-first authors.

B. Hong · Q. Huang · Y. Xu · X. Fang · Z. Li · J. Liu (✉)
Department of Neurosurgery, Changhai Hospital,
Second Military Medical University,
168 Changhai Road,
Shanghai 200433, China
e-mail: liujm8@163.com

K. Wang
Department of Neurosurgery,
General Hospital of Ji'nan Military Region,
Ji'nan 250031, China

## Materials and methods

### Animal experiment procedures

A total of 20 New Zealand white rabbits of both sexes (body weight 3–4 kg) were used in this experiment. Animals were given aspirin (10 mg/kg) and clopidogrel (10 mg/kg) orally every day from 3 days before to 28 days after the procedure, as described in the literature [10, 11]. Anesthesia was induced with an intramuscular injection of xylazine (12 mg/kg) and maintained with an intravenous injection of 1% pentobarbital sodium solution (10 mg/kg). The right femoral artery was isolated under sterile condition, and a 5-Fr (French) vascular sheath was inserted. Heparin (200 U/kg) was given by intravenous bolus injection, then a 5-Fr guiding catheter was placed into the abdominal aorta and digital subtraction angiography (DSA) was performed. The flow diversion device (Tubridge, Microport Medical, Shanghai, China) comprises 32 nickel–titanium alloy strands and two parallel platinum radio-opaque struts with a nominal MCR of 30–35%. The principle of choosing FD size was that the nominal diameter of stent was larger than the diameter of abdominal aorta, but no more than 1 mm. The device was advanced through a compatible microcatheter and placed in the abdominal aorta, covering at least one ostium of lumbar artery and, in some cases, also covering the renal artery ostium. DSA was performed again, before removal of the sheath and ligation of the femoral artery. Intravenous DSA (IVDSA) was performed 4 weeks after the procedure, and DSA was performed via left transfemoral access at 3 months. Based on the angiographic results, device morphology was examined and the patency of branches covered by the device was analyzed.

All experimental procedures were performed in accordance with the regulations set by the Animal Protection and Usage Committee of our university.

### Histological and pathological analysis

After the final angiography, the animals were sacrificed with an overdose of sodium pentobarbital, and the left ventricle was injected with 100 ml of 4% paraformaldehyde. The abdominal aorta with the device was explanted and trimmed. A 22 gauge intravenous catheter was advanced to the aorta, and both end of the aorta and branches were ligated. The tissue was perfused with 10% neutral buffered formalin for about 4 h at 100 cm of water column pressure, and then fixed in formalin for over 24 h. The tissue was washed with ethanol (50% V/V) and longitudinally cut into two halves, avoiding the ostia of the branches. After ethanol was fully evaporated, the branch ostia were examined under the stereo microscope and SEM under 40 Pa low vacuum conditions.

After SEM examination, tissue including branch ostium sites was cut into pieces about 3 mm in width and 10 mm in length, and the device mesh wires were carefully picked out under a stereo microscope. The specimen was embedded in paraffin and cut into 5-μm sections for hematoxylin and eosin (HE), Ponceau/Victoria blue (P/VB), and immunohistochemical staining with alpha smooth muscle actin (αSMA) and cluster of differentiation 68 (CD68).

### Data measurement and statistical analysis

Flow diversion device usage has been reported in the literature [1, 10, 21, 22], and the MCR can change as a result of either compression or stretching [3]. The MCR ($\varsigma$) of the device can be calculated according to the following formula:

$$\varsigma = \left[1 - \left(1 - nd\sqrt{\frac{1}{4A^2} + \frac{1}{\pi^2 D^2}}\right)^2\right] \times 100\%$$

where $n$ represents half of the wire number, $d$ stands for wire diameter of the device, $A$ and $D$ represent the distances between 16 consecutive wires along the long axis of the device and diameter of the device, respectively. All measured units are in millimeters. For the device used in our experiments, $n$ equals 16 and $d$ equals 0.05 mm. The detailed formula derivation will not be provided here.

Based on the SEM examination, the intimal coverage score was defined by the neointimal coverage ratio at the branch ostium: 1 point, the branch ostium coverage of neointima is less than or equal to 25%; 2 points, the branch ostium coverage of neointima is greater than 25% but less than or equal to 50%; 3 points, the branch ostium coverage of neointima is greater than 50% but less than or equal to 75%; 4 points, the branch ostium coverage of neointima is greater than 75%. The distances between 16 consecutive wires along the long axis of the device at the branch ostium and the diameter of the device under the stereo microscope were measured and used to calculate the MCR by the formula previously described (Fig. 1a).

On the P/VB-stained sections, except the branch ostia, the measurement between the neointima lumen edge and the internal elastic layer of the blood vessel within the device wires is considered to be the thickness of neointima. The $A$ value is double the measurement of the distance between eight consecutive wires, which is used together with the device diameter $D$ value measured under the stereo microscope to calculate the MCR using the formula (Fig. 1b).

The MCR and the intimal coverage scores between the renal artery and lumbar artery were compared using the nonparametric Mann–Whitney test. The relationship between the MCR of the device at the branch ostium and the neointimal coverage scoring was assessed by Spearman

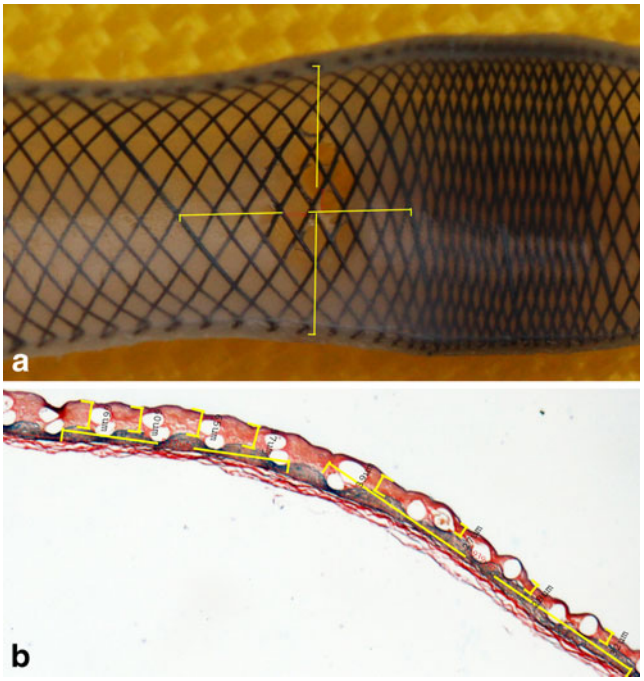


**Fig. 1** Measuring correlated indices to calculate the MCR. **a** Measuring the diameter and the distance between 16 consecutive wires along the long axis of the device at a branch ostium under stereo microscope. **b** Measuring thickness of neointima and the distance between eight consecutive wires on P/VB-stained sections. It was noted that the device wires were compressed or stretched after deployment

correlation analysis. The relationship between abdominal aorta neointimal thickness and device MCR was analyzed by Pearson correlation and linear regression. Average data were presented as mean±standard deviation. All statistical evaluations were made with the SPSS software (version 13.0, SPSS).

## Results

Except one animal whose lumbar artery ostium was not covered by the device due to technical reasons, a total of 19 lumbar artery and 10 renal artery ostia were covered by the device. No occlusion or delayed contrast filling of the device-covered branches was noted on angiographies immediately after FD implantation or at the follow-ups. There were no cases of significant stenosis within the device or displacement or kinking of the device at any follow-up time. Data relevant to the animals were summarized in Table 1.

No thrombosis was observed in the devices on gross or histological evaluation. SEM showed that there were more neointimal healings covering almost every strut and mesh at the edge of the branch artery ostia, but at the center, only sporadic fibrin deposits could be found on a minority of struts. There was also more neointimal covering at the proximal part of the ostia. The average MCR of the device

**Table 1** Data relevant to the experimental animals

| Animal | Diameter of artery prestent (mm) | Nominal diameter/ length of stent (mm) | Diameter of stent at branch orifice (mm) |
|---|---|---|---|
| 1 | 3.2 | 4/15 | 3.8(LA) |
| 2 | 3.8 | 4/15 | 4.1(LA) |
| 3 | 3.4 | 3.5/15 | N/A |
| 4 | 4 | 4/20 | 4.1(RRA), 3.4(LA) |
| 5 | 3.5 | 3.5/15 | 3.5(LA) |
| 6 | 3.4 | 4/15 | 4.1(LA) |
| 7 | 4 | 4/10 | 3.8(RRA), 3.7(LA) |
| 8 | 4 | 4.5/15 | 4.2 (RRA), 4.7(LA), 4.6 (LRA) |
| 9 | 3 | 3/15 | 3.1(LRA), 3(LA) |
| 10 | 3.8 | 4/15 | 4.1(LRA), 3.9(LA) |
| 11 | 3.1 | 4/15 | 4(LA) |
| 12 | 3.8 | 4/15 | 3.9(LA) |
| 13 | 3.2 | 4/15 | 3.8(LA) |
| 14 | 2.6 | 3/15 | 3.1(LA) |
| 15 | 3.5 | 4/15 | 3.5(LA) |
| 16 | 3.7 | 4/15 | 3.2(LRA), 3.2(LA) |
| 17 | 3.1 | 4/15 | 3.8(LRA), 3.6(LA) |
| 18 | 3.1 | 3.5/15 | 3.5(LA) |
| 19 | 3 | 4/15 | 4(LRA), 3.9(LA) |
| 20 | 3.9 | 4/15 | 3.8(LRA), 3.9(LA) |

*LA* Lumbar artery, *RRA* right renal artery, *LRA* left renal artery, *N/A* not applicable

at the ostia of the lumbar and renal arteries was 36.7±11.6% and 35.8±10.1%, respectively. There were no significant differences between these two kinds of branch arteries in terms of device coverage ($p$=0.902) and neointimal

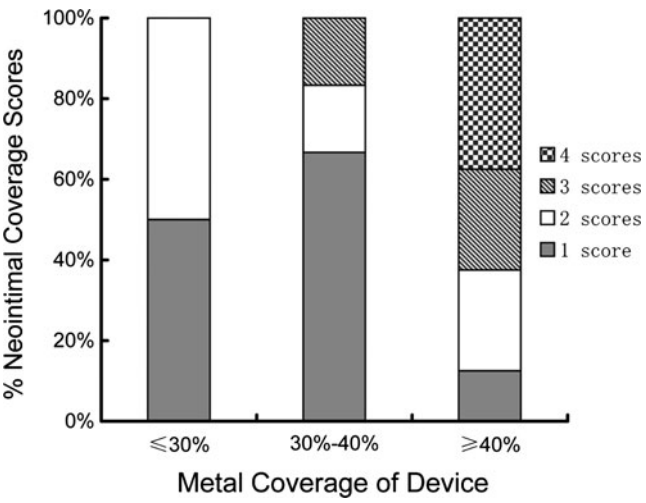


**Fig. 2** The intimal coverage scores of different MCR groups at branch ostia. MCR≥40% induces significantly more intimal coverage than the other two groups ($p$<0.05)

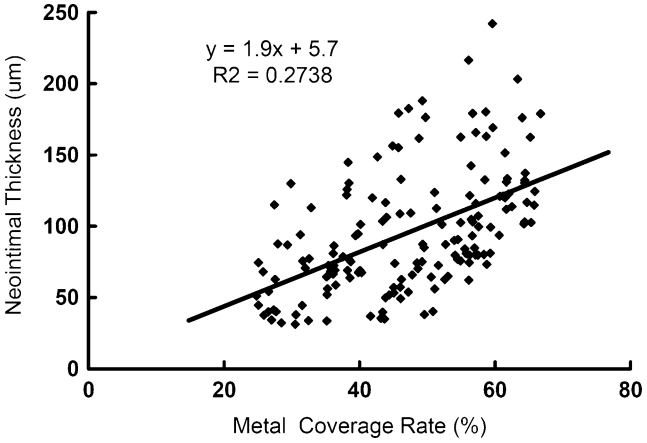


**Fig. 3** The correlation of an FD MCR and longitudinal section neointimal thickness. The higher the device MCR, the thicker the neointima is ($r$=0.523, $p$=0.001)

coverage scores ($p$=0.118). The overall MCR at the branch ostium covered by the device fell in the range of 23.5–49.6%, with an average of 36.4±10.8%. There was a positive correlation between intimal coverage score at the branch ostium and MCR ($r_s$=0.507, $p$=0.005). The MCRs at the renal artery and lumbar artery branch ostia could be divided into three groups: MCR≤30% (Group A), from 30% to 40% (Group B), and ≥40% (Group C). There was no significant difference of neointimal coverage scores of side branch artery ostia between groups A and B ($p$=0.792). But the neointimal coverage scores of group A and Group B were significantly lower than that of group C ($p$=0.021, Mann–Whitney test; Fig. 2).

We measured and analyzed the intimal thickness and the corresponding MCR of a total of 159 sets of sections from all of the device-treated animals. The neointimal thickness within the device struts was between 31 and 242 μm, with an average of 95±42 μm. The MCR was between 24.8% and 66.7%, with a mean coverage rate of 46.9±11.7%. There was also a positive correlation between neointimal thickness and device coverage ($r$=0.523, $p$=0.001, Fig. 3).

The representative pathological sections of branch ostia as well as their surrounding tissues were shown in Fig. 4. Vascular elastic fiber P/VB staining showed that the elastic layer was only located in the media; neointima did not exhibit an elastic layer (Fig. 1b). Neointima on the device struts was mainly composed of one to five layers of spindle

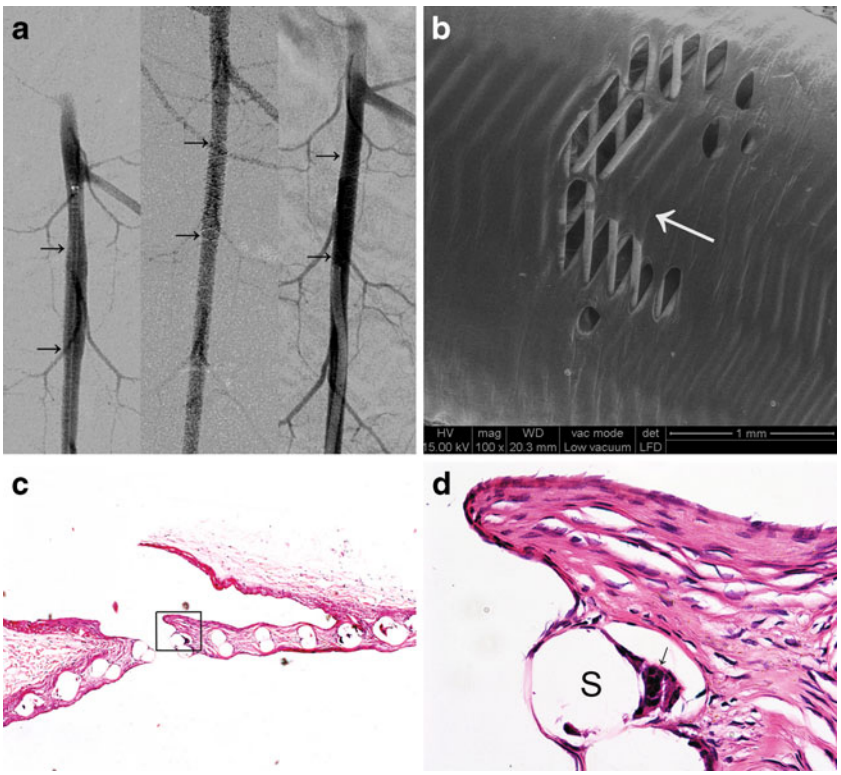


**Fig. 4** The imaging and pathology of rabbit abdominal aorta branch ostia covered by FD. **a** The angiography after abdominal aorta device implantation, immediately after (*left*), 4 weeks after (*middle*), and 3 months after shows that lumbar arteries covered by the device are still patent (*arrows* indicate the proximal and distal end of implanted FD). **b** SEM shows neointimal growth along the direction of blood flow (*white arrow*) at the lumbar artery ostium which is covered partly by device wires. **c** After removal of metal wires, the tissue is cut along the *white arrow* in **b** and stained with HE to show the lumbar artery ostium and the neointima (HE, ×50). **d** Enlarged view of **c** to show that the neointima surrounding device wires (*S*) is mainly composed of smooth muscle cells, collagen fibers, and multinuclear macrophages (*arrow*; HE, ×400)

cells. Immunohistochemical staining and HE staining showed that the neointima, including that located at the branch ostium, was mainly composed of α-actin-positive vascular smooth muscle cells and collagen. Polynuclear macrophages could be seen occasionally around the struts (Fig. 5).

## Discussion

With the publication of ISAT study [29, 30] and the advancement of technology and materials in the past two decades, interventional embolization is being used more frequently for intracranial aneurysm. Although balloon or stent-assisted coil embolization has made interventional treatment applicable to more aneurysms, fusiform and large or giant aneurysms still remain challenging. The application of FDs has provided a new treatment modality for these special types of intracranial aneurysms. Experimental work [2, 10, 11, 15–18, 22–25, 27, 31] and clinical application [5, 6, 13, 14, 20, 21, 26, 28] have been reported in recent years. High MCR and low porosity of the FDs are the major mechanisms to change the hemodynamic of aneurysm. In some clinical reports [5, 6, 13, 20, 21, 26], multiple FDs were implanted and overlapped to gain more MCR for stasis and thrombosis of aneurysms. However, the patency of side branches is a serious concern for the application of FDs, especially of multilayer overlapping. In the limited early clinical experiences, acute and late occlusion of side branches related to high metal coverage has been reported [13, 20, 21, 26]. Among the 19 aneurysm cases treated with pipeline FDs by Szikora et al. [26], the 6 months angiographic follow-up showed delayed occlusion of ophthalmic artery in two cases. Both branches that had delayed occlusion were covered by either two or four overlapping devices. Kulcsar et al. [13] used silk FDs to treat 12 cases of basilar artery aneurysm; among them, three had delayed ischemic attacks during a mean follow-up of 16 weeks. The acute infarction of tissue supplied by covered perforators may have been caused by thrombosis or excessive coverage of the branch ostia by device struts, whereas the delayed infarction may have been a result of excessive coverage and narrowing of the branch ostium by neointima overgrowth. In order to prevent the ischemic events of the perforator vessels, Szikora et al. [26] suggested avoiding overlapping device coverage of perforator vessels. Some researchers [1, 7–9] have designed asymmetrical FDs, the main purpose of which is to get enough coverage at the aneurysm neck while avoiding side effects of the diverting device on the side branches or perforators.

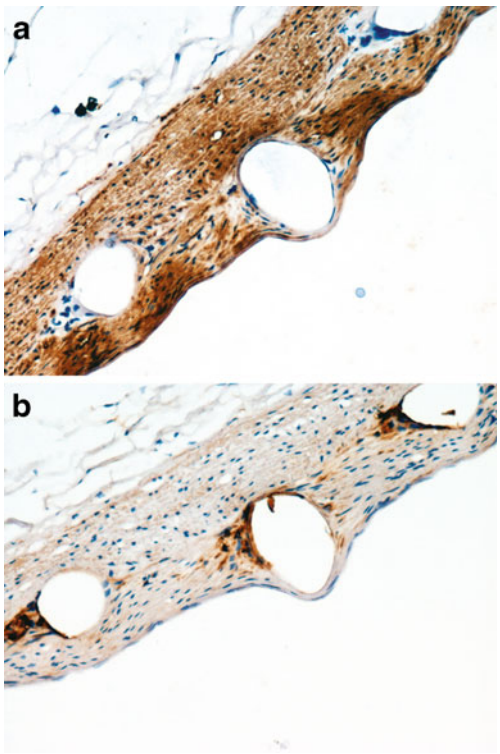


**Fig. 5** Immunohistochemical staining of rabbit abdominal aorta after removal of device. **a** αSMA-positive cells (*brown*) are located in the neointima and vascular media (IHC, ×200). **b** CD68-positive macrophages (*brown*) are located in the neointima and around the device mesh (IHC, ×200)

The MCR of the FD used for the treatment of aneurysm in current animal experiments was 30–35% [2, 10, 11, 13, 16, 22, 23]. In these experiments, no covered side branch occlusion was found in the follow-up angiography, but none of the experiments took into account the changes of the actual MCR in vivo. The MCR will change with curvature and diameter of the device relative to the diameter of the vessel in which it is placed [3]. It may also be influenced by different deployment manipulations such as pushing or pulling which may lead to compression or stretching of the devices. In this experiment, although the rabbit abdominal aorta was relatively straight and consistent in diameter, the actual MCR after FD implantation was still quite variable (23.5–49.6%, average 36.4±10.8%). Although the side branches covered by the FD were all patent at 3 months angiographic follow-up in our experiment, both pathology and SEM examination showed that the intimal coverage at the branch ostia changed with actual MCR. When the MCR was ≥40%, over 50% of intimal coverage was seen at the branch ostia, which was significantly higher than the other two groups with MCR less than 40%. Szikora et al. [26] also found that branches covered by single-layer FDs did not have acute or delayed side branch occlusion, while two cases of delayed side branch occlusion happened when covered with multilayer of FDs. Due to the design of the pipeline device, the MCR can be over 40% after two-layer coverage. From clinical reports and our results, multilayer

FD coverage of side branches or perforators may lead to ischemic events.

Our experiment showed that neointima at the branch ostia grew along the device struts and in the direction of blood flow. More neointima existed at the edge and proximal part of the ostium, whereas only fibrin deposits were found on the struts in the central part. Whether the neointima may continue to grow along the device struts with time is another question of concern.

Our experiment showed that neointimal thickness was positively related to the MCR. Therefore, whether excessive MCR will lead to stenosis inside the device is a matter of concern. The stents selected in this study had a diameter similar to that of the rabbit abdominal aorta, and this segment of rabbit abdominal aorta is relatively straight and consistent in diameter. Neointimal growth could be quite different when it was placed in the tortuous and inconsistently sized human intracranial vessels. Lylyk et al. [21] found that there was 8% (3/38) of mild to moderate in-stent stenosis (ISS) and 5% (2/38) of severe ISS at 3-month angiographic follow-up. In the 24 cases followed up by angiography by Lubicz et al. [20], significant parent artery stenosis at 6 months occurred in eight (33%), most of which (5 of 8) occurred when the distal end of the device was placed within an artery that had a significantly smaller diameter than that of the device. This may have been due to the high MCR and excessive intimal hyperplasia when FD was placed in a smaller artery. However, the model in this experiment was difficult to mimic the degree of bending and the different diameters of distal and proximal blood vessels found in the human brain. In the in vitro experiments of Aurboonyawat et al. [3], MCR increased significantly when FDs were placed in relatively small tubes. Therefore, it is worth further study of the actual MCR in small and bending blood vessels and the induced corresponding intimal hyperplasia after the implantation of FDs.

From our experimental results and other reports [10, 11, 22], tissue reactions to FDs are similar to the reported non-atherosclerotic arterial tissue reaction induced by coronary stents [32]. In the non-atherosclerotic blood vessels, neointima is mainly composed of smooth muscle cells, some monocytes and macrophages around the stent. In atherosclerotic blood vessels, the hyperplastic intima is mainly composed of large amounts of macrophages, smooth muscle cells, and new capillaries. Therefore, when we use a FD to treat an atherosclerotic aneurysm, the possibility of hyperplasia and perforator occlusion should be noted.

Our experiments do have some drawbacks. First, although literature has reported that the period of thrombosis, inflammation, and hyperplasia passes after 1 month following device implantation and the shaping period starts 3 months after the implantation [33]; this monitoring period might be too short for FDs. Second, the abdominal aorta used for implantation in this study cannot mimic the intracranial blood vessel bending and the diameter difference in the distal and proximal blood vessels. Third, pore density is another important factor which is not discussed in this study. Animal experiments with different pore densities and MCRs for longer follow-up periods are needed for future studies.

**Acknowledgments** This work was supported by the National Natural Science Foundation of China (30973102, 30901556) and Rising-Star Program of Shanghai Science and Technology Committee (grant no. 11QA1408400). We gratefully thank MicroPort Medical (Shanghai) for the free flow-diverting stents.

**Conflict of interest** We declare that we have no conflict of interest.

## References

1. Ahlhelm F, Roth C, Kaufmann R, Schulte-Altedorneburg G, Romeike BF, Reith W (2007) Treatment of wide-necked intracranial aneurysms with a novel self-expanding two-zonal endovascular stent device. Neuroradiology 49:1023–1028
2. Augsburger L, Farhat M, Reymond P, Fonck E, Kulcsar Z, Stergiopulos N, Rufenacht DA (2009) Effect of flow diverter porosity on intraaneurysmal blood flow. Klin Neuroradiol 19:204–214
3. Aurboonyawat T, Blanc R, Schmidt P, Piotin M, Spelle L, Nakib A, Moret J (2011) An in vitro study of silk stent morphology. Neuroradiology 53:659–667
4. Aurboonyawat T, Schmidt PJ, Piotin M, Blanc R, Spelle L, Moret J (2011) A study of the first-generation pipeline embolization device morphology using intraoperative angiographic computed tomography (ACT). Neuroradiology 53:23–30
5. Fiorella D, Kelly ME, Albuquerque FC, Nelson PK (2009) Curative reconstruction of a giant midbasilar trunk aneurysm with the pipeline embolization device. Neurosurgery 64:212–217
6. Fiorella D, Woo HH, Albuquerque FC, Nelson PK (2008) Definitive reconstruction of circumferential, fusiform intracranial aneurysms with the pipeline embolization device. Neurosurgery 62:1115–1120
7. Ionita CN, Dohatcu A, Sinelnikov A, Sherman J, Keleshis C, Paciorek AM, Hoffmann KR, Bednarek DR, Rudin S (2009) Angiographic analysis of animal model aneurysms treated with novel polyurethane asymmetric vascular stent (P-AVS): feasibility study. Proc Soc Photo Opt Instrum Eng 7262:72621H72621–72621H72610
8. Ionita CN, Paciorek AM, Dohatcu A, Hoffmann KR, Bednarek DR, Kolega J, Levy EI, Hopkins LN, Rudin S, Mocco JD (2009) The asymmetric vascular stent: efficacy in a rabbit aneurysm model. Stroke 40:959–965
9. Ionita CN, Paciorek AM, Hoffmann KR, Bednarek DR, Yamamoto J, Kolega J, Levy EI, Hopkins LN, Rudin S, Mocco J (2008) Asymmetric vascular stent: feasibility study of a new low-porosity patch-containing stent. Stroke 39:2105–2113
10. Kallmes DF, Ding YH, Dai D, Kadirvel R, Lewis DA, Cloft HJ (2007) A new endoluminal, flow-disrupting device for treatment of saccular aneurysms. Stroke 38:2346–2352
11. Kallmes DF, Ding YH, Dai D, Kadirvel R, Lewis DA, Cloft HJ (2009) A second-generation, endoluminal, flow-disrupting device for treatment of saccular aneurysms. AJNR Am J Neuroradiol 30:1153–1158
12. Kim M, Taulbee DB, Tremmel M, Meng H (2008) Comparison of two stents in modifying cerebral aneurysm hemodynamics. Ann Biomed Eng 36:726–741

13. Kulcsar Z, Ernemann U, Wetzel SG, Bock A, Goericke S, Panagiotopoulos V, Forsting M, Ruefenacht DA, Wanke I (2010) High-profile flow diverter (silk) implantation in the basilar artery: efficacy in the treatment of aneurysms and the role of the perforators. Stroke 41:1690–1696
14. Kulcsar Z, Wetzel SG, Augsburger L, Gruber A, Wanke I, Andre Rufenacht D, Sadasivan C, Cesar L, Seong J, Rakian A, Hao Q, Tio FO, Wakhloo AK, Lieber BB, Fujimura N, Ohta M, Abdo G, Ylmaz H, Lovblad KO, Rufenacht DA (2009) Effect of flow diversion treatment on very small ruptured aneurysms. Neurosurgery 67:789–793
15. Lieber BB, Livescu V, Hopkins LN, Wakhloo AK (2002) Particle image velocimetry assessment of stent design influence on intra-aneurysmal flow. Ann Biomed Eng 30:768–777
16. Lieber BB, Sadasivan C (2010) Endoluminal scaffolds for vascular reconstruction and exclusion of aneurysms from the cerebral circulation. Stroke 41(10 Suppl):S21–25
17. Lieber BB, Stancampiano AP, Wakhloo AK (1997) Alteration of hemodynamics in aneurysm models by stenting: influence of stent porosity. Ann Biomed Eng 25:460–469
18. Liou TM, Li YC (2008) Effects of stent porosity on hemodynamics in a sidewall aneurysm model. J Biomech 41:1174–1183
19. Liou TM, Li YC, Wang TC (2008) Hemodynamics altered by placing helix stents in an aneurysm at a 45 degrees angle to the curved vessel. Phys Med Biol 53:3763–3776
20. Lubicz B, Collignon L, Raphaeli G, Pruvo JP, Bruneau M, De Witte O, Leclerc X (2010) Flow-diverter stent for the endovascular treatment of intracranial aneurysms: a prospective study in 29 patients with 34 aneurysms. Stroke 41:2247–2253
21. Lylyk P, Miranda C, Ceratto R, Ferrario A, Scrivano E, Luna HR, Berez AL, Tran Q, Nelson PK, Fiorella D (2009) Curative endovascular reconstruction of cerebral aneurysms with the pipeline embolization device: the Buenos Aires experience. Neurosurgery 64:632–642
22. Sadasivan C, Cesar L, Seong J, Rakian A, Hao Q, Tio FO, Wakhloo AK, Lieber BB (2009) An original flow diversion device for the treatment of intracranial aneurysms: evaluation in the rabbit elastase-induced model. Stroke 40:952–958
23. Sadasivan C, Cesar L, Seong J, Wakhloo AK, Lieber BB (2009) Treatment of rabbit elastase-induced aneurysm models by flow diverters: development of quantifiable indexes of device performance using digital subtraction angiography. IEEE Trans Med Imaging 28:1117–1125
24. Sadasivan C, Lieber BB, Cesar L, Miskolczi L, Seong J, Wakhloo AK (2006) Angiographic assessment of the performance of flow divertors to treat cerebral aneurysms. Conf Proc IEEE Eng Med Biol Soc 1:3210–3213
25. Seong J, Wakhloo AK, Lieber BB (2007) In vitro evaluation of flow divertors in an elastase-induced saccular aneurysm model in rabbit. J Biomech Eng 129:863–872
26. Szikora I, Berentei Z, Kulcsar Z, Marosfoi M, Vajda ZS, Lee W, Berez A, Nelson PK (2010) Treatment of intracranial aneurysms by functional reconstruction of the parent artery: the Budapest experience with the pipeline embolization device. AJNR Am J Neuroradiol 31:1139–1147
27. Szikora I, Nelson PK, Berentei Z, Kulcsar Z, Marosfoi M, Berez A (2008) The potential of flow modification in the treatment of intracranial aneurysms. Interv Neuroradiol 14(Suppl 1):77–80
28. van Rooij WJ, Sluzewski M (2010) Perforator infarction after placement of a pipeline flow-diverting stent for an unruptured A1 aneurysm. AJNR Am J Neuroradiol 31:E43–E44
29. Molyneux AJ, Kerr RS, Birks J, Ramzi N, Yarnold J, Sneade M, Rischmiller J (2009) Risk of recurrent subarachnoid haemorrhage, death, or dependence and standardised mortality ratios after clipping or coiling of an intracranial aneurysm in the international subarachnoid aneurysm trial (ISAT): long-term follow-up. Lancet Neurol 8:427–433
30. Molyneux AJ, Kerr RS, Yu LM, Clarke M, Sneade M, Yarnold JA, Sandercock P (2005) International subarachnoid aneurysm trial (ISAT) of neurosurgical clipping versus endovascular coiling in 2143 patients with ruptured intracranial aneurysms: a randomised comparison of effects on survival, dependency, seizures, rebleeding, subgroups, and aneurysm occlusion. Lancet 366:809–817
31. Rhee K, Han MH, Cha SH (2002) Changes of flow characteristics by stenting in aneurysm models: influence of aneurysm geometry and stent porosity. Ann Biomed Eng 30:894–904
32. Komatsu R, Ueda M, Naruko T, Kojima A, Becker AE (1998) Neointimal tissue response at sites of coronary stenting in humans: macroscopic, histological, and immunohistochemical analyses. Circulation 98:224–233
33. Edelman ER, Rogers C (1998) Pathobiologic responses to stenting. Am J Cardiol 81:4E–6E